

Supporting Information

Optimizing supramolecular fluorescent materials with responsive multi-color tunability toward soft biomimetic skins

*Muqing Si,^{†ab} Huihui Shi,^{†ab} Hao Liu,^{ab} Hui Shang,^a Guangqiang Yin,^{ab} Shuxin Wei,^{ab} Shuangshuang Wu,^{ab} Wei Lu^{*ab} and Tao Chen^{*ab}*

- a.* Key Laboratory of Marine Materials and Related Technologies Zhejiang Key Laboratory of Marine Materials and Protective Technologies, Ningbo Institute of Materials Technology and Engineering, Chinese Academy of Sciences, Ningbo 315201, China.
- b.* School of Chemical Sciences, University of Chinese Academy of Sciences, Beijing 100049, China.

Contents

1. Experimental Procedures	S-3
1.1 Materials	S-3
1.2 Synthesis of the methyl 6-(3-(2-(methacryloyloxy) ethyl) ureido) picolinate (MAUP).....	S-3
1.3 Synthesis of fluorescent copolymer.....	S-3
1.4 Preparation of Eu/Tb-PHNVC/PHM film	S-4
1.5 Self-healing of Eu/Tb-PHNVC/PHM film.....	S-4
1.6 Preparation of soft biomimetic skin for camouflage and display.	S-5
1.7 Characterization.....	S-5
2. Results and Discussion.....	S-7
Figure S1. Synthetic procedure of MAUP.....	S-7
Figure S2. ¹ H NMR spectrum of MAUP	S-8
Figure S3. ¹³ C NMR spectrum of MAUP	S-9
Figure S4. ESI-MS spectrum of MAUP	S-10
Figure S5. ¹ H NMR spectrum of PHM.....	S-11
Figure S6. FTIR spectrum of PHM.....	S-12
Figure S7. GPC curve of PHM	S-13
Figure S8. Fitting analysis of ¹ H NMR spectrum of PHM.....	S-14
Table S1. Fitting results of ¹ H NMR spectrum of PHM.....	S-14
Figure S9. UV-vis spectra of MAUP and PHM	S-15
Figure S10. UV-vis calibration curve MAUP as a function of its concentration	S-16
Figure S11. Fabrication process of the Eu-PHM film.....	S-17
Figure S12. Transmittance spectra of PHM and Eu-PHM.....	S-18
Figure S13. Fluorescence spectra of Eu ³⁺ solution, MAUP-Eu ³⁺ complex solution and Eu-PHM film	S-19
Figure S14. Corresponding classification of N atoms in PHM and Eu-PHM of XPS spectra	S-20
Figure S15. High-resolution XPS fitting results for O 1s spectra of PHM and Eu-PHM film	S-21
Figure S16. Humidity-dependent fluorescence spectra of the Eu-PHM films with different [Eu ³⁺]/[MAUP]	S-22
Figure S17. Digital photos of Eu/Tb-PHM with various Eu ³⁺ /Tb ³⁺ molar ratio and relative humidity	S-23
Figure S18. Fluorescence spectra of Tb-PHM in response to humidity change and its comparison with Eu-PHM	S-24
Figure S19. ¹ H NMR spectrum of PHNVC.....	S-25
Figure S20. FTIR spectrum of PHNVC.....	S-26
Figure S21. GPC curve of PHNVC.....	S-27
Figure S22. UV-vis spectrum of PHNVC.....	S-28
Figure S23. UV-vis calibration curve NVC as a function of its concentration.....	S-29
Figure S24. Fluorescence spectra of the PHNVC film recorded at different humidity.....	S-30
Figure S25. Transmittance spectra of the PHNVC/PHM film and Eu-PHNVC/PHM film	S-31
Figure S26. SEM images of cross section of Eu-PHNVC/PHM film	S-32
Figure S27. SEM images of corresponding EDS mapping region.....	S-33
Figure S28. Optimizing of the PHNVC content in the fluorescent polymeric films	S-34
Figure S29. Fluorescence spectra and CIE diagram of the Tb/Eu-PHNVC/PHM film in response to humidity change	S-35
Figure S30. Color-change of the supramolecular polymer films in response to pH changes.....	S-36
Figure S31. Color-change of the supramolecular polymer films in response to light	S-37
Figure S32. Color-change of the supramolecular polymer films in response to temperature.....	S-38
Figure S33. Digital photos, fluorescent spectra and CIE diagram of the Eu-PHNVC/PHM film in response to consecutive Tb ³⁺ and Eu ³⁺ stimulus.....	S-39
Figure S34. Strain–stress curve and tearing curve of Eu-PHNVC/PHM film.....	S-40

Figure S35. 2D Young's modulus distributions of PHM film, TFA-PHM film, and the Eu-PHNVC/PHM film	S-41
Figure S36. In situ microscopic image of self-healing of Eu-PHNVC/PHM film	S-42
Figure S37. Control experiment showing the importance of high humidity to self-healing	S-43
Figure S38. Digital photos showing the self-healing process of the man-made morpho butterfly	S-44
Figure S39. Digital photos showing the artificial system designed to mimic the dazzling and colorful pattern change of the morpho butterfly	S-45
Figure S40. Digital photos of hiding and display of the information loaded on the chameleon robot	S-46
3. Reference	S-47

1. Experimental Procedures

1.1 Materials

Dimethyl sulfoxide (DMSO, 99.0%), dimethyl formamide (DMF, 99.9%), Tb(NO₃)₃·5H₂O (99.9%), N-vinyl carbazole (NVC, 98%), lithium chloride (LiCl, 98%), magnesium chloride (MgCl₂, 99.9%), sodium bromide (NaBr, 99%) and potassium sulfate (K₂SO₄, 99%), trifluoromethanesulfonic acid (TFA, 99%) were purchased from Aladdin Chemistry Co. Ltd. Sodium chloride (NaCl, 99%), potassium chloride (KCl, 99%), methanol (99%), ethanol (99%), hydrochloric acid (HCl, F.W. 36.46, 99%), ammonia solution (NH₃, F.W. 17.03, 99%), filter papers and pan papers were obtained from Sinopharm Chemical Reagent Co. Ltd. N-(2-hydroxyethyl)acrylamide (HEAA, 98%, stabilized with MEHQ) was provided by Shanghai Macklin Biochemical Co. Ltd. Methyl 6-Aminopyridine-2-carboxylate (98.0%) and Eu(NO₃)₃·6H₂O (99.9%) were supplied by Energy Chemical. Dichloromethane (99.9%, Superdry), 2,2'-azoisobutyronitrile (AIBN, 99%) were gotten from J&K Scientific Ltd. 2-isocyanatoethyl methacrylate (98%) was purchased from TCI (Shanghai) Development Co., Ltd. AIBN was purified through recrystallization and vacuum distillation. HEAA passed through an alumina column to remove stabilizer before use. Other materials were used without further purification.

1.2 Synthesis of the methyl 6-(3-(2-(methacryloyloxy)ethyl)ureido)picolinate (MAUP)

Under N₂ protection, 6-aminopyridine-2-carboxylate (15 g, 0.098 mol) was dissolved in dry dichloromethane (100 mL), followed by the dropwise addition of a mixture solution of dichloromethane (25 mL) and 2-isocyanatoethylmethacrylate (15.5 g, 0.10 mol) in the ice water bath. The reaction mixture was kept stirring for 48 h at room temperature and then the solvent was removed by rotary evaporation. The crude products were then washed by 200 mL saturated NaHCO₃ aqueous solution and filtered out, subsequently dried in vacuum for 48 h. After aforementioned steps, 28.12 g (92.2%) white powder was obtained. No toxic raw material was used and no harmful chemical was produced during the synthetic process. All wasted chemicals were carefully collected, classified and disposed according to experiment guidelines and regulations. ¹H NMR (400 MHz, DMSO-d₆) δ 9.67 (s, 1H), 8.21 (s, 1H), 7.83 (t, J = 7.9 Hz, 1H), 7.59 (dd, J = 10.2, 7.8 Hz, 2H), 6.01 (s, 1H), 5.62 (t, J = 1.7 Hz, 1H), 4.14 (t, J = 5.4 Hz, 2H), 3.81 (s, 3H), 3.45 (q, J = 5.5 Hz, 2H), 1.82 (s, 3H) (**Figure S2**). ¹³C NMR (101 MHz, DMSO-d₆) δ 166.94, 165.10, 155.16, 153.66, 144.73, 139.82, 136.24, 126.28, 118.42, 115.95, 64.00, 52.84, 38.69, 18.33 (**Figure S3**). MS (ESI) m/z for C₁₄H₁₇N₃O₅ [M-H]⁺ calculated: 308.12, found: 308.12 (**Figure S4**).

1.3 Synthesis of fluorescent copolymer

1.3.1 Synthesis of poly(N-(2-hydroxyethyl)acrylamide-co-methyl 6-(3-(2-(methacryloyloxy)ethyl)ureido)picolinate) (PHM)

Under N₂ protection, MAUP (fluorescent monomer, 1 g), HEAA (monomer, 7 g) and AIBN (initiator, 0.08 g) were dissolved in DMSO (29 mL). The reaction was carried out in 70 °C for 8 h. The obtained organogel

were then immersed into ethanol to remove DMSO and unreacted monomers. The ethanol was refreshed every 12 h for 4 times. Next, the products were immersed into deionized water, which was refreshed every 12 h for 4 times, for solvent replacement, followed by vacuum freeze-drying for 48h to afford final products. After aforementioned steps, 7.16 g (89.5%) white solid was obtained. No toxic raw material was used and no harmful chemical was produced during the synthetic process. All wasted chemicals were carefully collected, classified and disposed according to experiment guidelines and regulations. ^1H NMR (400 MHz, $\text{DMSO-}d_6$) δ 7.60 (s, 4H), 5.03 (s, 1H), 4.97 (s, 1H), 4.93 – 4.86 (m, 1H), 4.77 (s, 1H), 3.86 (s, 1H), 3.46 – 3.40 (m, 6H), 3.25 (s, 3H), 3.09 (s, 5H), 2.97 (s, 1H), 2.54 (s, 2H), 2.02 (s, 1H), 1.86 (s, 3H), 1.50 (s, 2H), 1.31 (s, 6H). FTIR spectra: the PHM film shows peaks at 1249 cm^{-1} , 1648 cm^{-1} , which are attributed to the stretching vibration of the C-O-C, the C=O of ester groups. The peaks locate at 2935 cm^{-1} and 1544 cm^{-1} corresponds to the C=O of urea groups and the C-H of pyridine in MAUP, respectively. The characteristic O-H peak of HEAA shows at 1390 cm^{-1} . Molecular weight determination: $M_w = 1.20 \times 10^5$, $M_n = 3.7 \times 10^4$, polydispersity index (PDI) = 3.270.

1.3.2 Synthesis of poly(N-(2-hydroxyethyl) acrylamide-co-N-vinyl carbazole) (PHNVC)

Under N_2 protection, NVC (fluorescent monomer, 2 g), HEAA (monomer, 0.593 g), AIBN (initiator, 0.026 g) were dissolved in DMSO (20 mL). The reaction was kept in $70\text{ }^\circ\text{C}$ for 8 h, followed by precipitate the product in 500 mL ethanol. Finally, the products were dried in vacuum for 8 h to get PHNVC. After aforementioned steps, 0.746 g (28.8%) faint yellow solid was obtained. No toxic raw material was used and no harmful chemical was produced during the synthetic process. All wasted chemicals were carefully collected, classified and disposed according to experiment guidelines and regulations. ^1H NMR (400 MHz, $\text{DMSO-}d_6$) δ 7.04 (s, 3H), 6.56 (s, 1H), 4.95 (s, 1H), 1.53 (s, 3H). FTIR spectra: peaks at 1452 cm^{-1} and 750 cm^{-1} belong to C=C vibration and C-H bending in benzene, which strongly indicates the presents of carbazole group. Overtones of benzene also ranges from 1716 cm^{-1} to 2000 cm^{-1} . The characteristic O-H peak of HEAA shows at 1332 cm^{-1} . Molecular weight determination: $M_w = 1.24 \times 10^5$, $M_n = 4.3 \times 10^4$, polydispersity index (PDI) = 2.897.

1.4 Preparation of Eu/Tb-PHNVC/PHM film

Mixture of PHM, PHNVC and $\text{Eu}^{3+}/\text{Tb}^{3+}$ nitrate in specific ratio was dissolved in DMF. The obtained solution was added into PTFE mold and the DMF was evaporated at $60\text{ }^\circ\text{C}$ for 20 h. Sheet-like Ln-PHNVC/PHM composite film was peeled off manually from the mold and further dried in the vacuum oven at $25\text{ }^\circ\text{C}$ for 24 h.

1.5 Self-healing of Eu/Tb-PHNVC/PHM film

To begin with, the rectangular Eu-PHNVC/PHM film was cut into two pieces for following self-healing experiment. The edges of these two parts were brought into contact and placed into sealed chamber with inner RH at 98% for 4 h. When the film was brought back to normal environment (e.g., RH~60%), the film was healed completely without distinguishable edges, which was further confirmed by microscope (**Figure S36**). The healed film was sufficiently stable to resist external force (**Movie S1**).

1.6 Preparation of soft biomimetic skin for camouflage and display.

1.6.1 Preparation of soft biomimetic skin for camouflage

The soft biomimetic skin for camouflage was prepared by adhering tailored Eu-PHNVC/PHM film with pan paper in environment at RH=98%. Both layers will not split up during bending and the pan paper show no influence on the fluorescence of Eu-PHNVC/PHM film. Then the obtained bilayer film was pasted to chameleon robot by VHB tape with Eu-PHNVC/PHM film on the outside.

1.6.2 Preparation of soft biomimetic skin for display

The soft biomimetic skin for display was prepared by layer-by-layer integration of Tb-PHNVC/PHM film, VHB tape, the green luminous paper with pre-coded information. The green luminous paper was prepared from pan paper coated with green fluorescent paint and tailored into desired shape.

1.7 Characterization

^1H NMR and ^{13}C NMR measurements

^1H NMR and ^{13}C NMR spectra were obtained from a Bruker Avance III 400 MHz spectrometer, operated at 400.0 MHz for the proton nuclei.

ESI-MS measurements

ESI-MS spectra were gathered from an AB Sciex TripleTOF 4600.

High Temperature Gel Permeation Chromatography (GPC)

Molecular weight averages of aforementioned polymer were measured at 80 °C on a TOSOH HLC8320 gel permeation chromatograph (GPC) equipped with refractive index detector (RI). Dimethylformamide (DMF) was utilized as the eluent at a flowing rate of 0.6 mL/min, and a series of commercial poly(methyl methacrylate) (PMMA) standards were employed to calibrate the GPC elution traces.

UV-Vis absorption and transmittance measurements

UV-Vis absorption and transmittance spectra were measured on an UV-Vis spectrophotometer (TU-1810, Purkinje General Instrument Co., Ltd.).

ATR-FTIR characterization

ATR-FTIR spectra was recorded on a Thermo Scientific Nicolet 6700 FT-IR spectrometer with 32 scans, spanning a spectral range of 4000–400 cm^{-1} with a resolution of 4.0 cm^{-1} .

Digital photos taken under UV light

The digital photos of the polymeric films were taken under a UV lamp (ZF-5, 8 W, 254 nm). All fluorescent photographs were taken using the same UV lamp.

Fluorescence measurements

Steady-state fluorescence measurements were obtained from a Hitachi F-4600 fluorescence spectrofluorometer at room temperature with a 500 W Xenon lamp. The excitation wavelength was 254 nm and the scan speed was 1200 nm min⁻¹. Saturated salt aqueous solutions were used for humidity control.

SEM and EDS mapping characterization

The surface EDS mapping and cross section morphology of the polymeric film were performed by a field-emission scanning electron microscopy (SEM, S-4800, Hitachi) with an accelerating voltage of 8.0 kV.

XPS characterization

The chemical bonding and bonding state were measured by XPS using a Kratos AXIS ULTRADLD instrument with a monochromic Al K α X-ray source (hv=1486.6 eV).

Polarizing microscope characterization

Microscopic images were obtained from an OLYMPUS BX51 polarizing microscope.

Mechanical test

The mechanical test sample was prepared by cutting the Eu-PHM/PHNVC film into sheet-like samples (gauge length of 35 mm, width of 2 mm, and thickness of 0.03 mm). Mechanical tensile test was performed using a Zwick Z1.0 electromechanical dynamometer under ambient conditions of ~60% relative humidity at 25 °C with a strain rate of 5 mm min⁻¹. Each measurement was repeated at least three times. For tearing test, a 0.5 mm wide crack perpendicular to the stretching direction was applied on each sample and tested at a tensile rate of 5 mm min⁻¹ under ambient conditions of ~60% relative humidity at 25 °C. Each measurement was repeated at least three times. The tearing energy (Γ) could be calculated according to the following formula: $\Gamma = HW(\lambda_{cr})$, where $W(\lambda_{cr})$ is the elastic energy density of the uncut sample the before critical stretch λ_{cr} (critical stretch λ_{cr} is the λ of the sample with a precut crack recorded at fracture), and H is the height of the sample in the undeformed state.¹

Nanomechanical mapping measurements

Nanomechanical mapping measurements of Eu-PHNVC/PHM samples were conducted using Dimension ICON (Bruker, USA) in a PeakForce tapping mode.

2. Results and Discussion

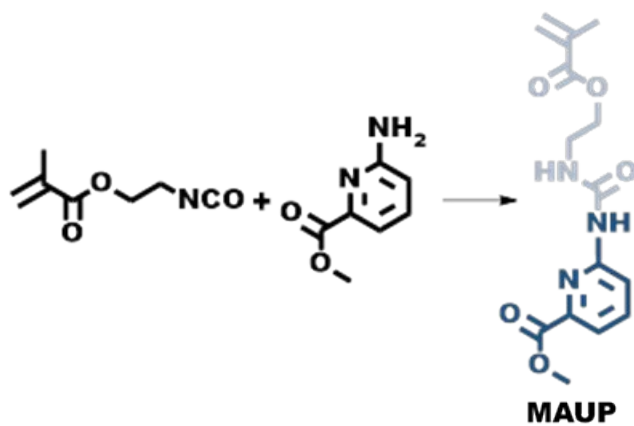


Figure S1. Synthetic procedure of MAUP.

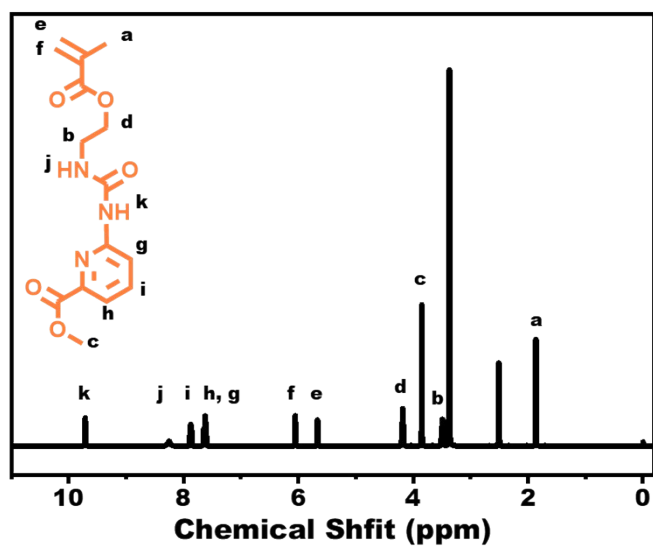


Figure S2. ¹H NMR spectrum of MAUP in DMSO-d₆.

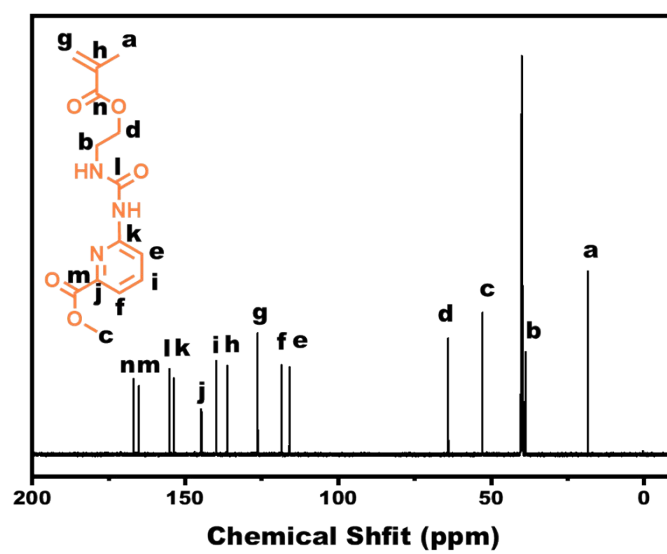


Figure S3. ^{13}C NMR spectrum of MAUP in DMSO-d_6 .

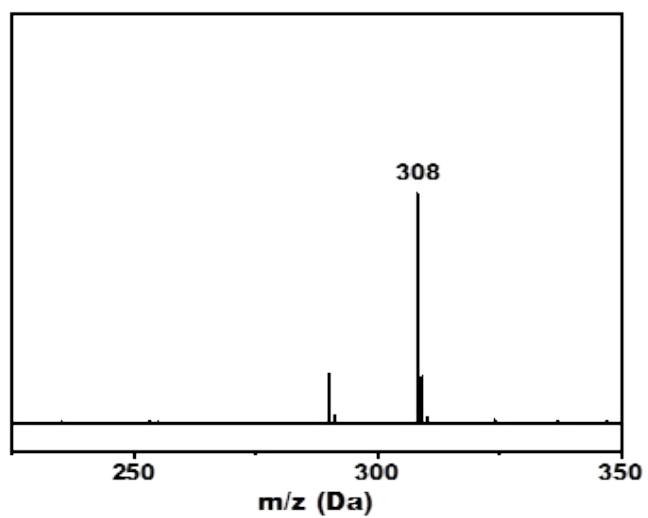


Figure S4. ESI-MS spectrum of MAUP. The spectrum revealed the molecular weight of as-synthetic molecular to be 307, which is in accordance to the designed molecule.

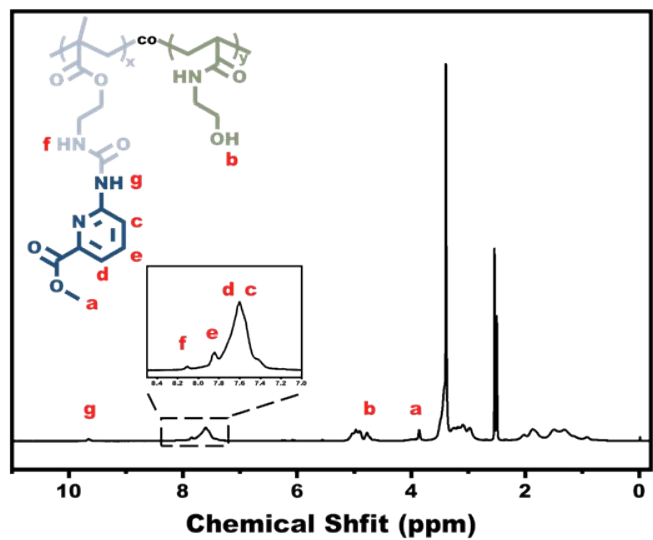


Figure S5. ¹H NMR spectrum of PHM in DMSO-d₆.

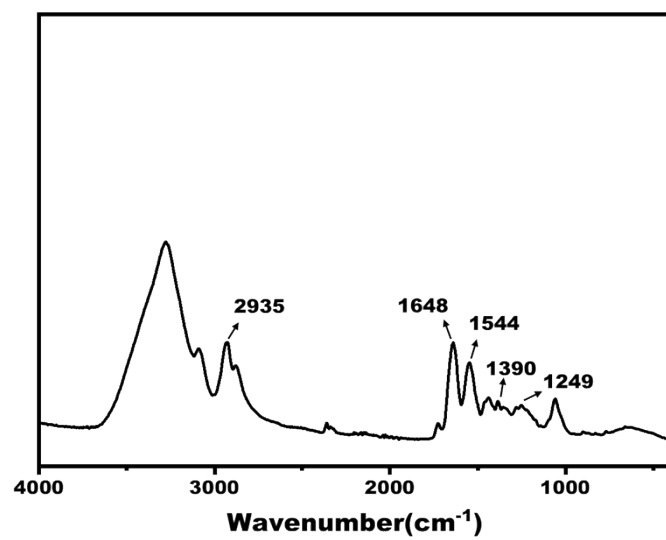


Figure S6. FTIR spectrum of PHM.

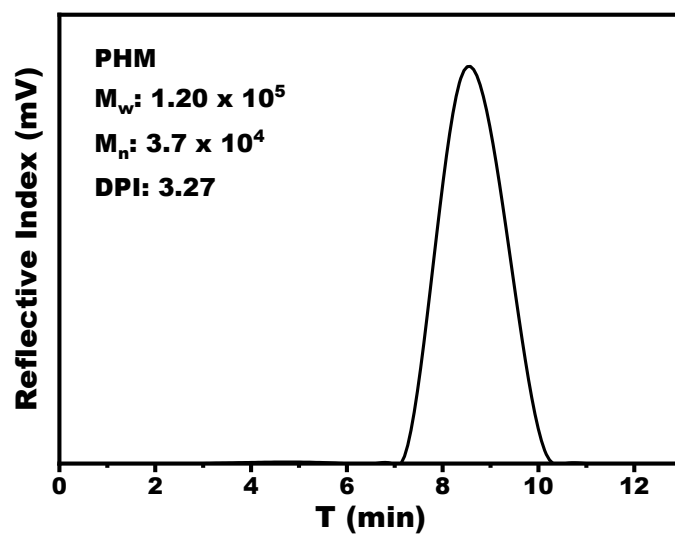


Figure S7. GPC curve of PHM in DMF.

The method used to calculate the MAUP content in PHM according to ^1H NMR spectroscopy.

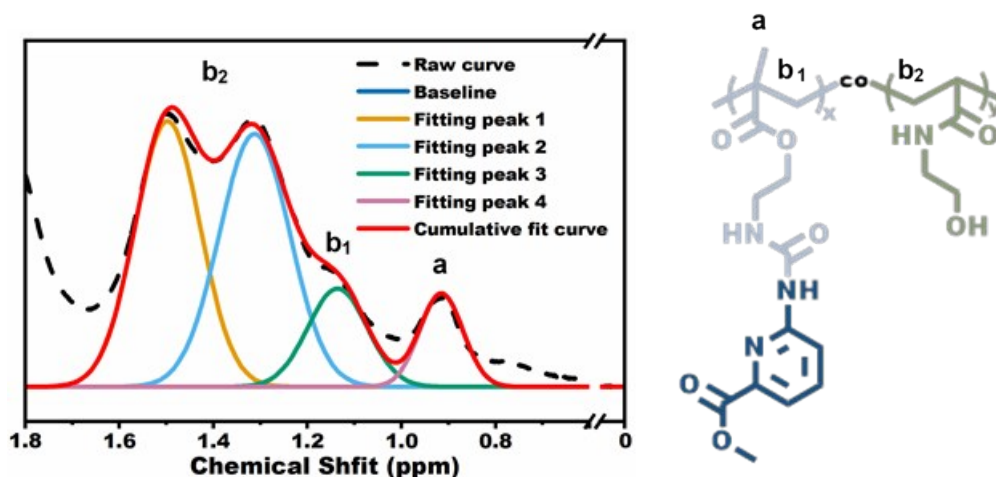


Figure S8. Fitting analysis of ^1H NMR spectrum of PHM in DMSO-d_6 .

Table S1. Fitting results of ^1H NMR spectrum of PHM in DMSO-d_6 .

Peak index	Area integral	FWHM (ppm)	Center (ppm)
1	66.5325	0.1628	1.4974
2	68.6858	0.1765	1.3124
3	22.4351	0.1484	1.1362
4	15.5133	0.1080	0.9155

As can be seen from the molecular formula of PHM, the methyl group on the main chain only belongs to MAUP while the methylene group belongs to both MAUP and HEAA. In addition, as can be seen from **Figure S8**, fitting peak a, fitting peak b_1 and fitting peak b_2 correspond to methyl group of MAUP, methylene group of MAUP and methylene group of HEAA, respectively. Thus, the MAUP content can be calculated from equation as below:

$$C_{MAUP} = I_a / (I_{b_1} + I_{b_2})$$

where I_a , I_{b_1} and I_{b_2} are the integral of the area under fitting peak a, fitting peak b_1 and fitting peak b_2 , respectively. As a result, molar ratio of HEAA/MAUP in PHM was calculated to be 15.2:1 from ^1H NMR spectrum using fitting analysis.

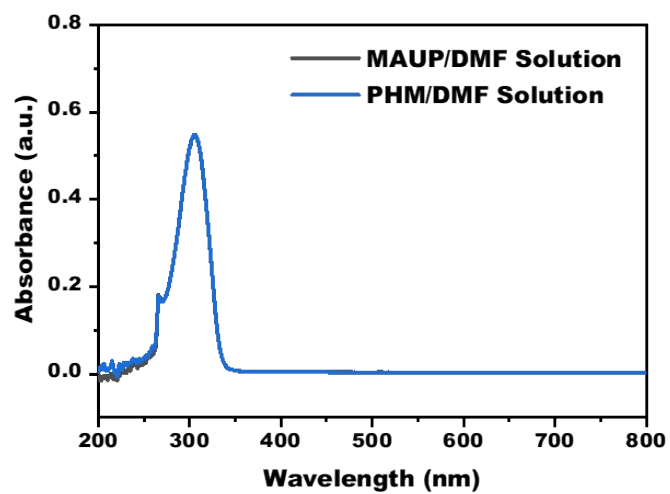


Figure S9. UV-vis spectra of MAUP (1.12×10^{-4} M) and PHM (0.24 mg/mL).

The method used to calculate the MAUP content in PHM by UV-vis calibration curve

A calibration curve of absorbance at 306 nm versus MAUP concentration (in DMF) was created, and the optical path of the quartz cell was 10 mm. Then 25 mg PHM was dissolved into 50 mL DMF. The absorbance of obtained solution was 0.99, indicating the molar concentration of the solution to be 2.17×10^{-4} M. In other word, there were $2.17 \times 10^{-4} \times 10^{-3} \times 50 = 10.85 \times 10^{-6}$ mol MAUP in 25 mg copolymers. Thus, the mass ratio and molar ratio between HEAA and MAUP in copolymers were 6.2:1 and 17.2:1, respectively.

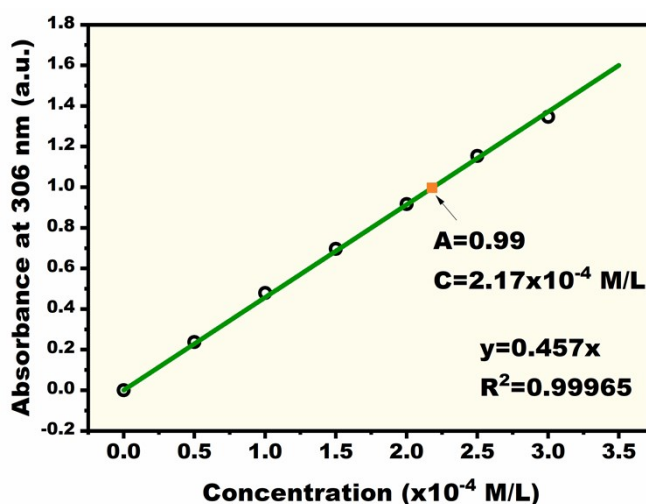


Figure S10. Calibration curve showing the absorbance of MAUP at 306 nm as a function of its concentration. Square point indicates the absorbance of 0.5 mg/mL PHM/DMF solution.

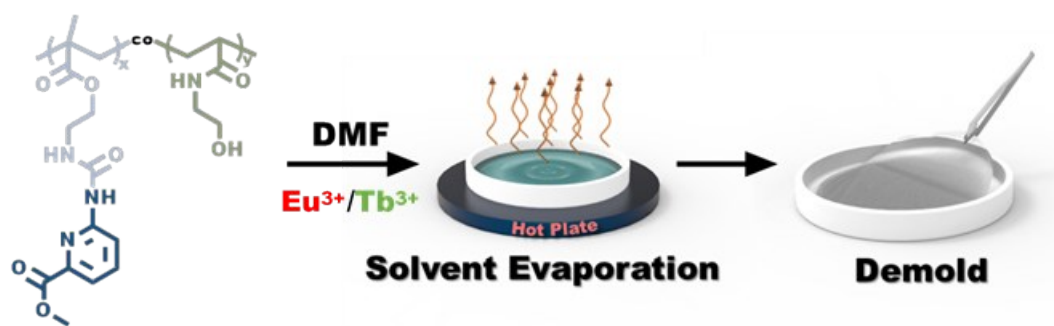


Figure S11. Schematic illustration showing the fabrication process of the Eu/Tb-PHM film.

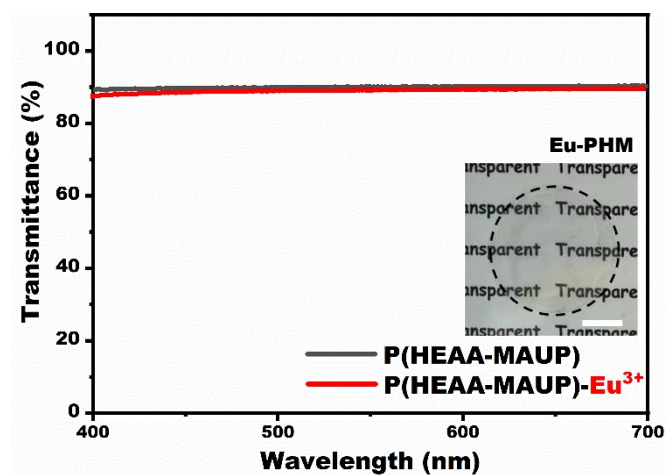


Figure S12. The transmittance spectra of PHM and Eu-PHM. Insert photo shows Eu-PHM film under day light (Scale bar is 5 mm).

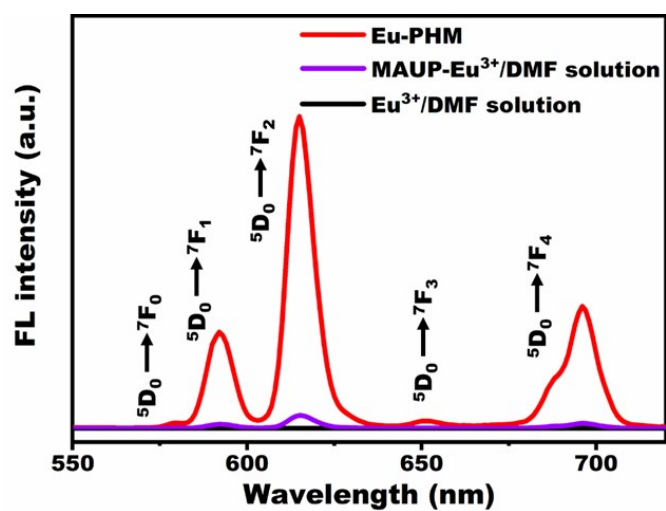


Figure S13. Fluorescence spectra of Eu³⁺ solution (2.17×10^{-4} M, in DMF), MAUP-Eu³⁺ complex solution (0.5 mg/mL, in DMF) and the Eu-PHM film. MAUP-Eu³⁺ solution and Eu-PHM film was prepared with $[\text{Eu}^{3+}]/[\text{MAUP}]=1:3$. Excitation at 254 nm.

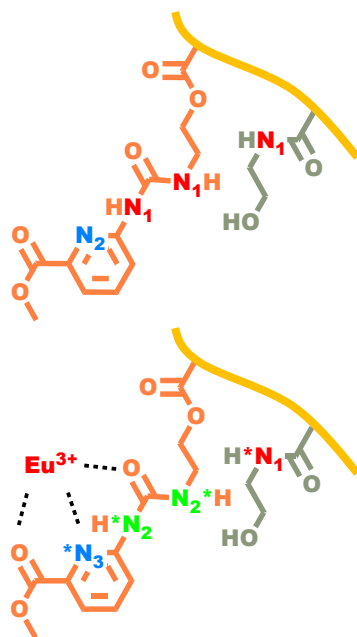


Figure S14. Corresponding classification of N atoms in PHM and Eu-PHM of XPS N 1s spectra.

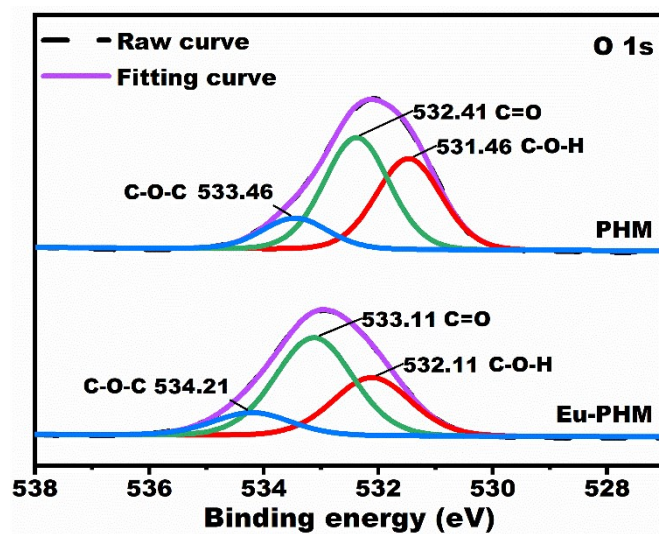


Figure S15. High-resolution XPS fitting results for O 1s spectra of PHM and Eu-PHM film.

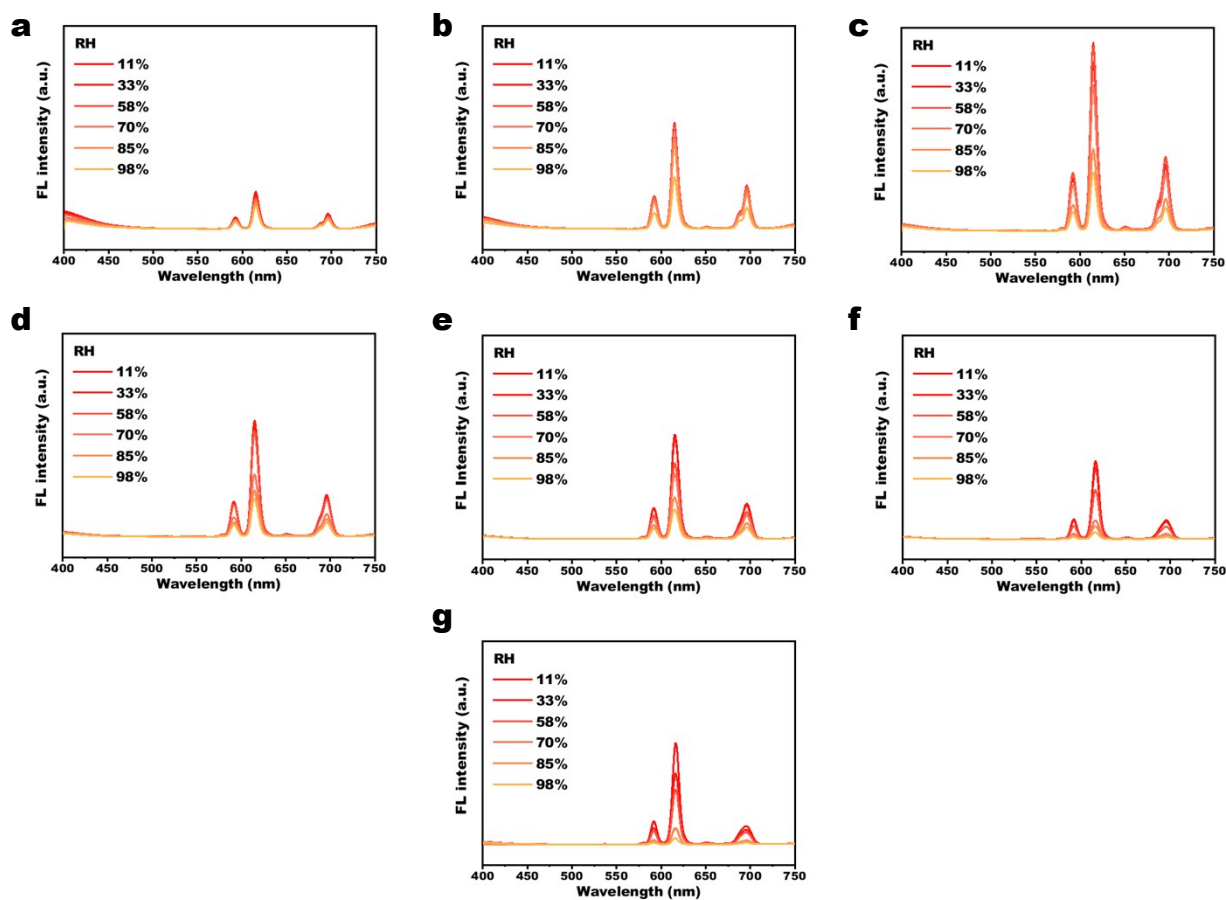


Figure S16. Humidity-dependent fluorescence spectra of the Eu-PHM films with $[\text{Eu}^{3+}]/[\text{MAUP}] = 0.05$ a), 0.1 b), 0.3 c), 0.5 d), 1 e), 3 f), 5 g). (Insert digital photos show corresponding Eu-PHM film at RH=11% (left) and RH=98% (right)). Excitation at 254 nm. All photos were taken under a 254 nm UV lamp.

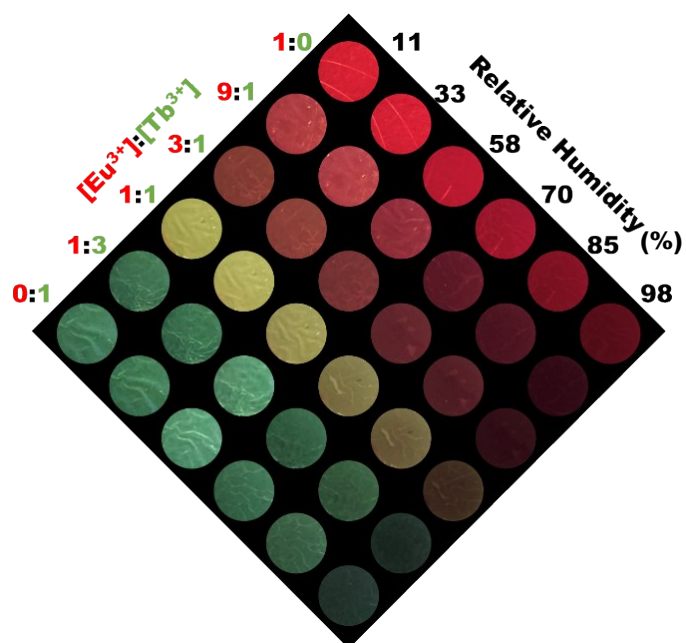


Figure S17. Digital photos of Eu/Tb-PHM with various Eu^{3+}/Tb^{3+} molar ratio and relative humidity. All photos were taken under a 254 nm UV lamp.

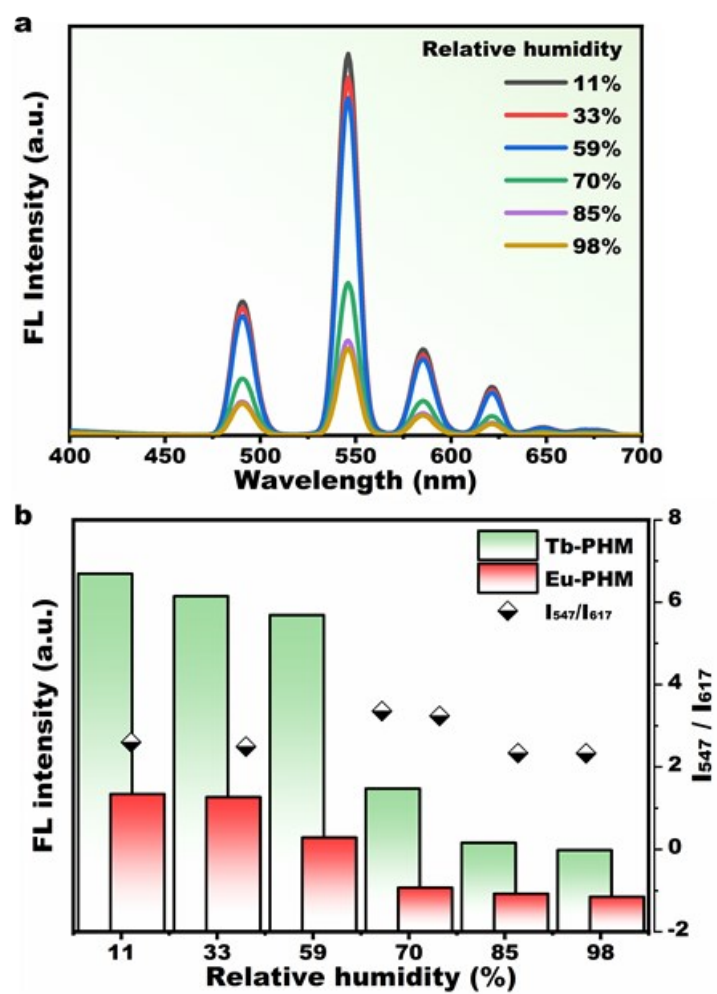


Figure S18. a) Fluorescence spectra of Tb-PHM in response to humidity change. b) Fluorescent intensity of Eu-PHM at 617 nm, fluorescent intensity of Tb-PHM at 547 nm and the ratio between them as a function of relative humidity. Excitation at 254 nm.

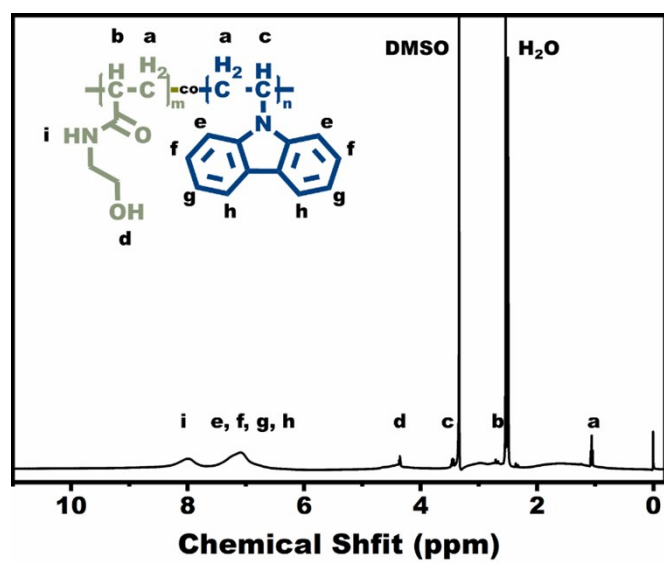


Figure S19. ¹H NMR spectrum of PHNVC in DMSO-d₆.

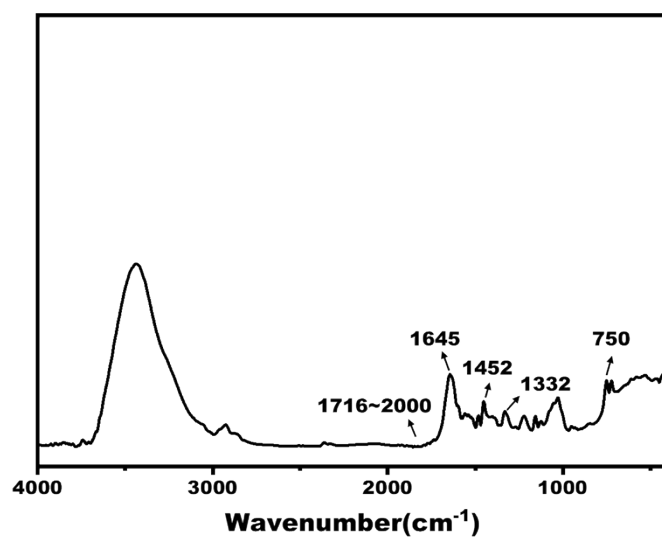


Figure S20. FTIR spectrum of PHNVC.

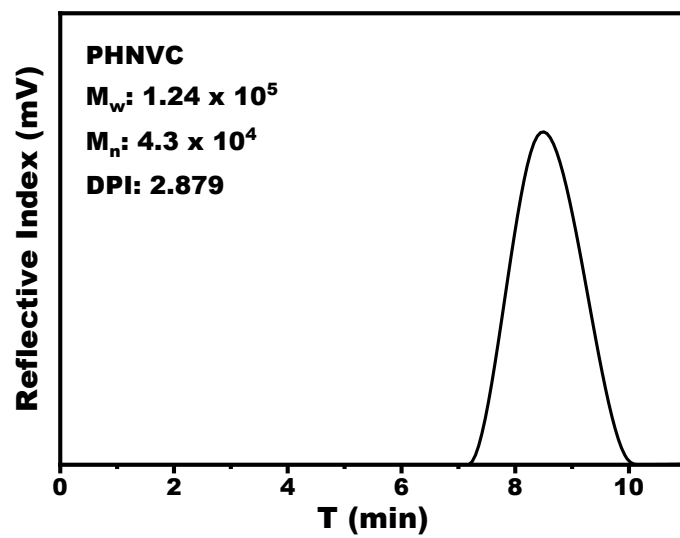


Figure S21. GPC curve of PHNVC in DMF.

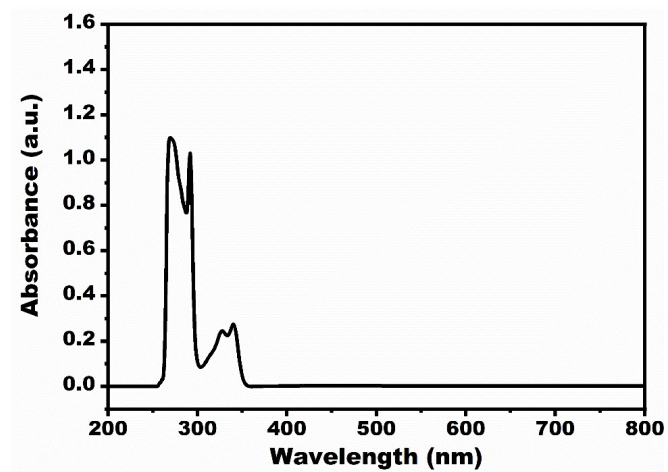


Figure S22. UV-vis spectrum of PHNVC (0.21 mg/mL).

Determination of molar ratio of NVC content in PHNVC by UV-vis calibration curve

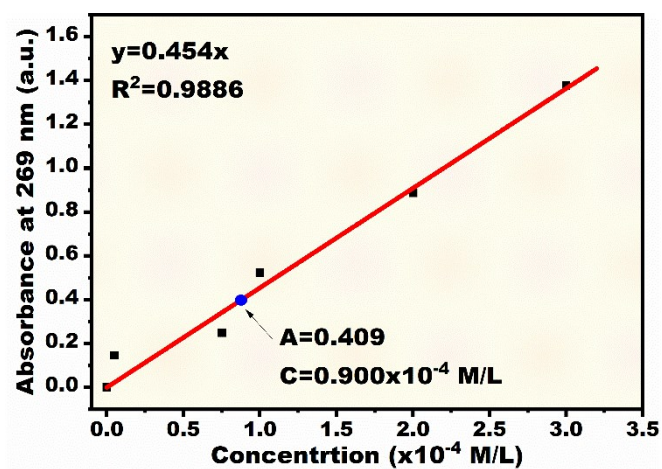


Figure S23. Calibration curve for determining NVC concentration. Blue point indicates the absorbance of tested PNVC/DMF solution. Determination of molar ratio of HEAA to NVC in PHNVC was conducted by the same method as aforementioned calibration of molar ratio of MAUP content in PHM. This calibration curve was constructed for the absorption at a wavelength of 269 nm and the optical path of the quartz cell was 10 mm. Solution for tested were 0.13 mg/mL PHNVC/DMF solution.

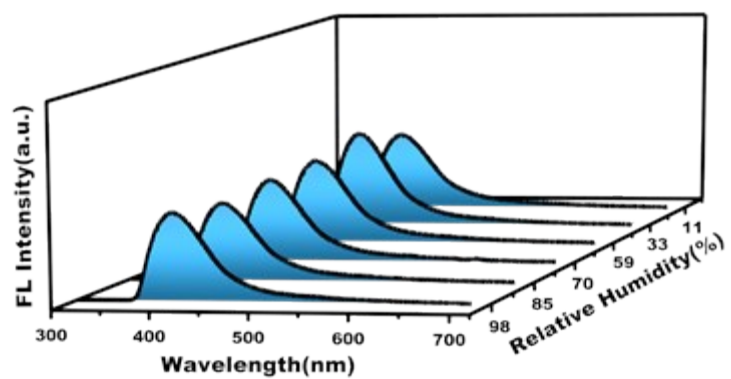


Figure S24. Fluorescence spectra of the PHNVC film recorded at different humidity. Excitation at 254 nm.

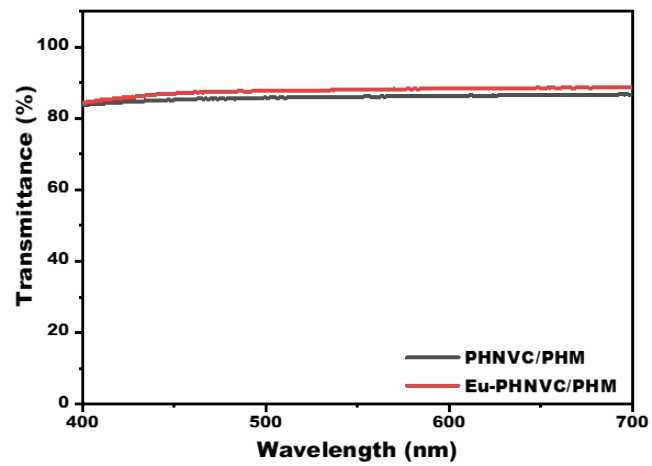


Figure S25. The transmittance spectra of the PHNVC/PHM film and Eu-PHNVC/PHM film.

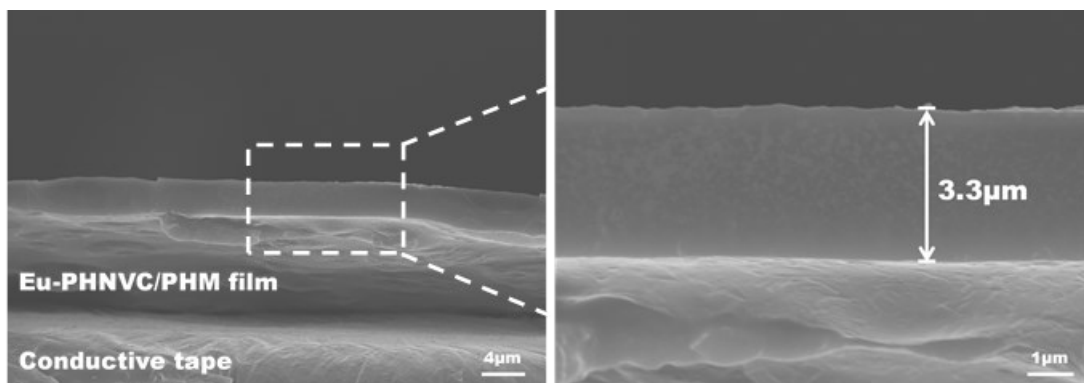


Figure S26. SEM image of cross section of Eu-PHNVC/PHM film, which reveals the thickness of the Eu-PHNVC/PHM film to be 3.3 µm.

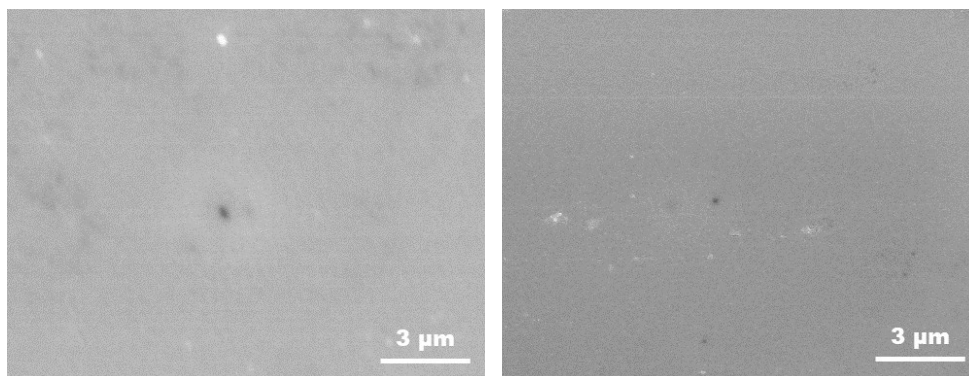


Figure S27. SEM images of corresponding energy dispersive X-ray spectroscopy (EDS) mapping region of the Eu-PHNVC/PHM film (left) and Tb-PHNVC/PHM film (right).

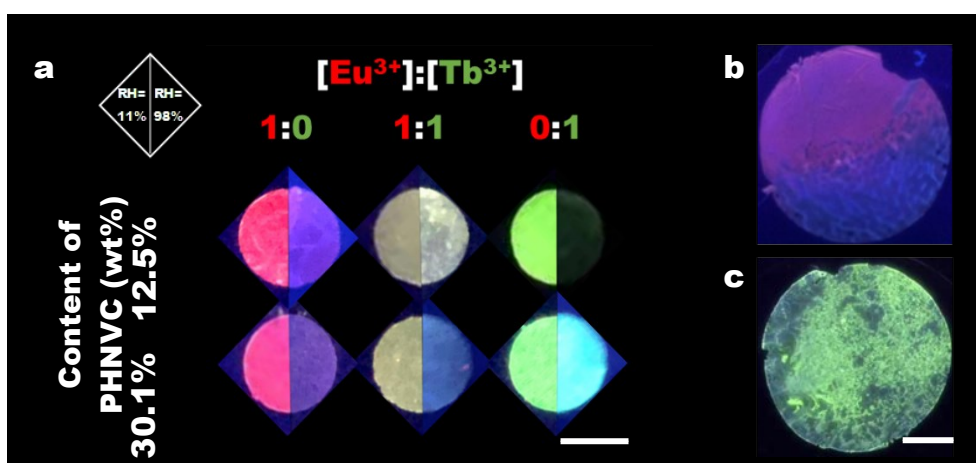


Figure S28. a) Digital photos of the Eu/Tb-PHNVC/PHM films at RH=11% and RH=98% (Scale bar is 3 mm). If the PHNVC content reaches 55.0%, severe phase isolation happens, leading to the inhomogeneous films. Photos of the Eu-PHNVC/PHM and Tb-PHNVC/PHM films with the PHNVC content of 55.0% are shown in b) and c) (Scale bar is 5 mm). All photos were taken under a 254 nm UV lamp.

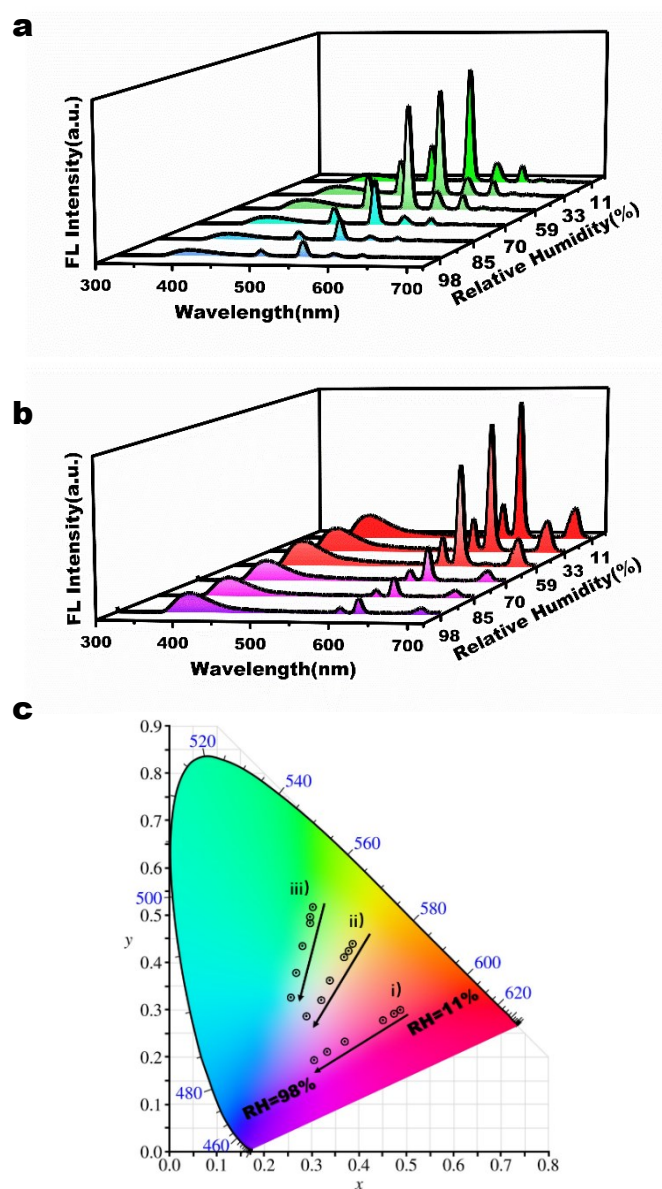


Figure S29. Fluorescence spectra of a) the Tb-PHNVC/PHM film and b) Eu-PHNVC/PHM film in response to humidity change. c) CIE diagram for humidity-triggered color changing process of i) Eu-PHNVC/PHM, ii) Eu/Tb-PHNVC/PHM ($\text{Eu}^{3+}/\text{Tb}^{3+}=1:1$) and iii) Tb-PHNVC/PHM. Excitation at 254 nm.

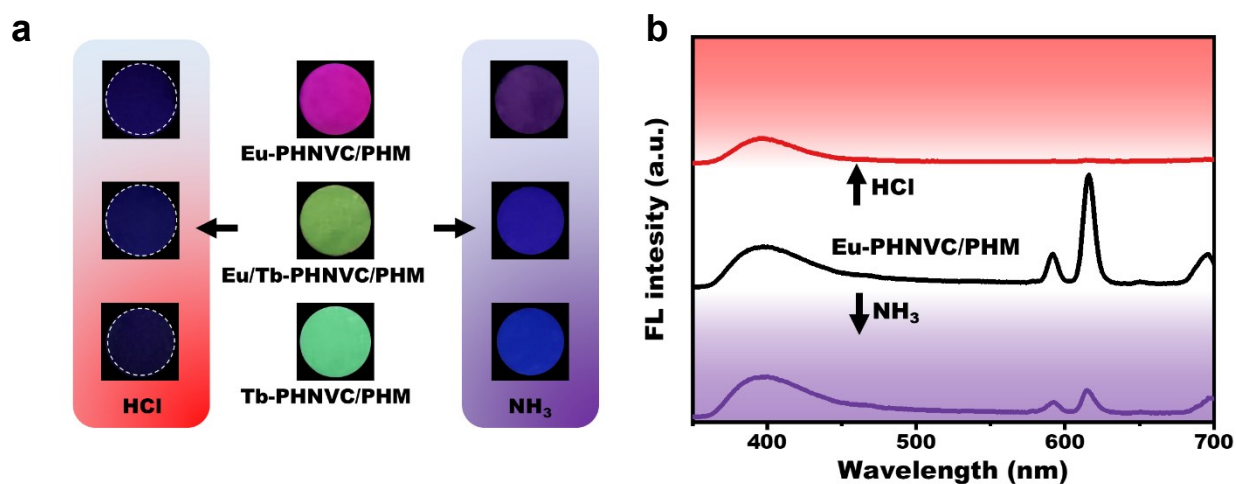


Figure S30. a) Digital photos showing the color change of the Eu-PHNVC/PHM film, Eu/Tb-PHNVC/PHM film (Eu/Tb=1:1), and Tb-PHNVC/PHM film in response of pH changes. The photographs were taken under a 254 nm UV lamp. b) Fluorescent spectrum of Eu-PHNVC/PHM film at 617 nm before and after being exposed to HCl and NH₃. Excitation at 254 nm.

As summarized in **Figure S30**, upon exposure to acid/base stimuli (e.g., HCl/NH₃), the red fluorescence of Eu-PHNVC/PHM film gradually changed to be blue or purple. This is because the red-light-emitting Eu-MAUP complexes could be decomposed by these acid/base chemicals.²⁻⁴ Similarly, pH-responsive yellow-to-blue and green-to-blue emission color changes were observed for the Eu/Tb-PHNVC/PHM film and Tb-PHNVC/PHM film, respectively.

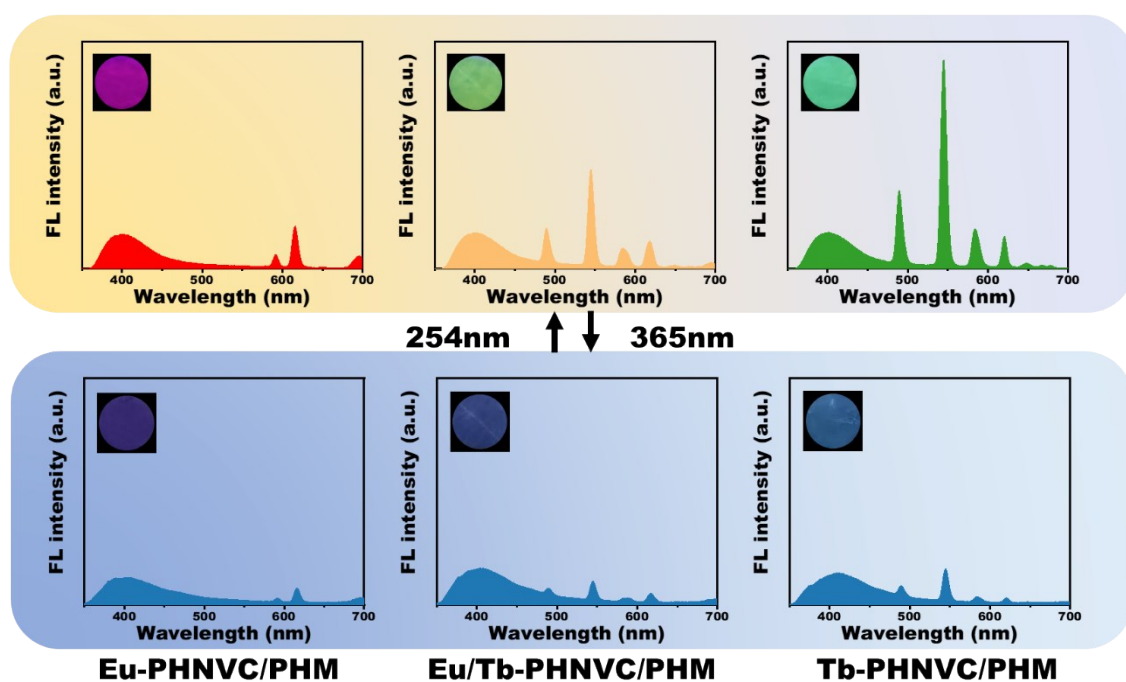


Figure S31. Fluorescent spectrum and digital photos of the Eu-PHNVC/PHM film, Eu/Tb-PHNVC/PHM film (Eu/Tb=1:1), and Tb-PHNVC/PHM film under different excitation light.

Excitation light dependent fluorescence color changes demonstrated by these films are shown in **Figure S31**. Red-to-blue, yellow-to-blue and green-to-blue emission color changes were observed for the Eu-PHNVC/PHM film, Eu/Tb-PHNVC/PHM film and Tb-PHNVC/PHM film, respectively. These results can be easily understood for the following reasons. As reported in the previous papers and illustrated in **Figure S22**, the blue fluorescent carbazole moieties have a primary absorption band ranges from 247 nm to 370 nm and thus exhibit blue light emission when excited at either 365 nm or higher-energy 254 nm UV light.⁵ By contrast, the red/green fluorescent Eu/Tb-MAUP complexes were only highly red-light-emitting when excited at 254 nm, but nearly non-fluorescent under lower-energy 365 nm light excitation, because the picolinate chromophore has only a small conjugation unit that has no absorbance band above 350 nm (**Figure S11**).

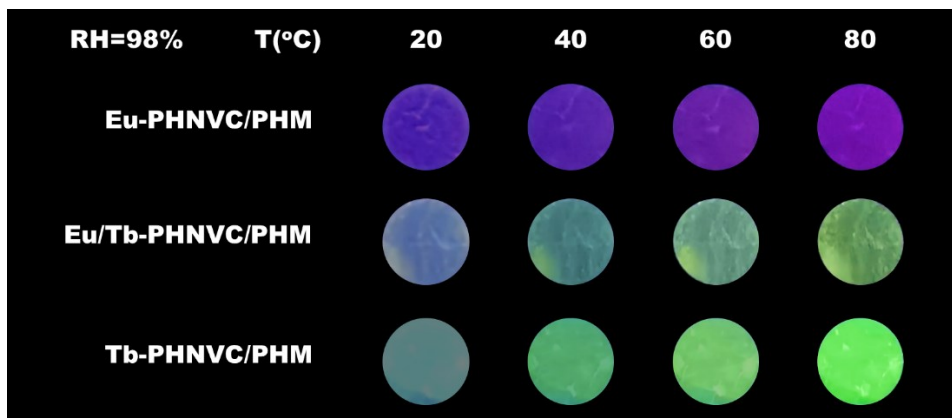


Figure S32. Digital photos showing the fluorescent color change of Eu-PHNVC/PHM film, Eu/Tb-PHNVC/PHM film (Eu/Tb=1:1), and Tb-PHNVC/PHM film in response to temperature changes under constant RH=98%. The photographs were taken under a 254 nm UV lamp.

Temperature-triggered emission color change can be realized under constant humidity, because the environmental humidity can be easily regulated by the environmental temperature change.^{6,7} There, it is feasible to regulate the color of humidity-responsive Eu/Tb-PHNVC/PHM by varying environmental temperature. **Figure S32** demonstrates the temperature-triggered purple-to-red, blue-to-yellow, and cyan-to-green fluorescent color change of Eu-PHNVC/PHM film, Eu/Tb-PHNVC/PHM film (Eu/Tb=1:1), and Tb-PHNVC/PHM film, respectively.

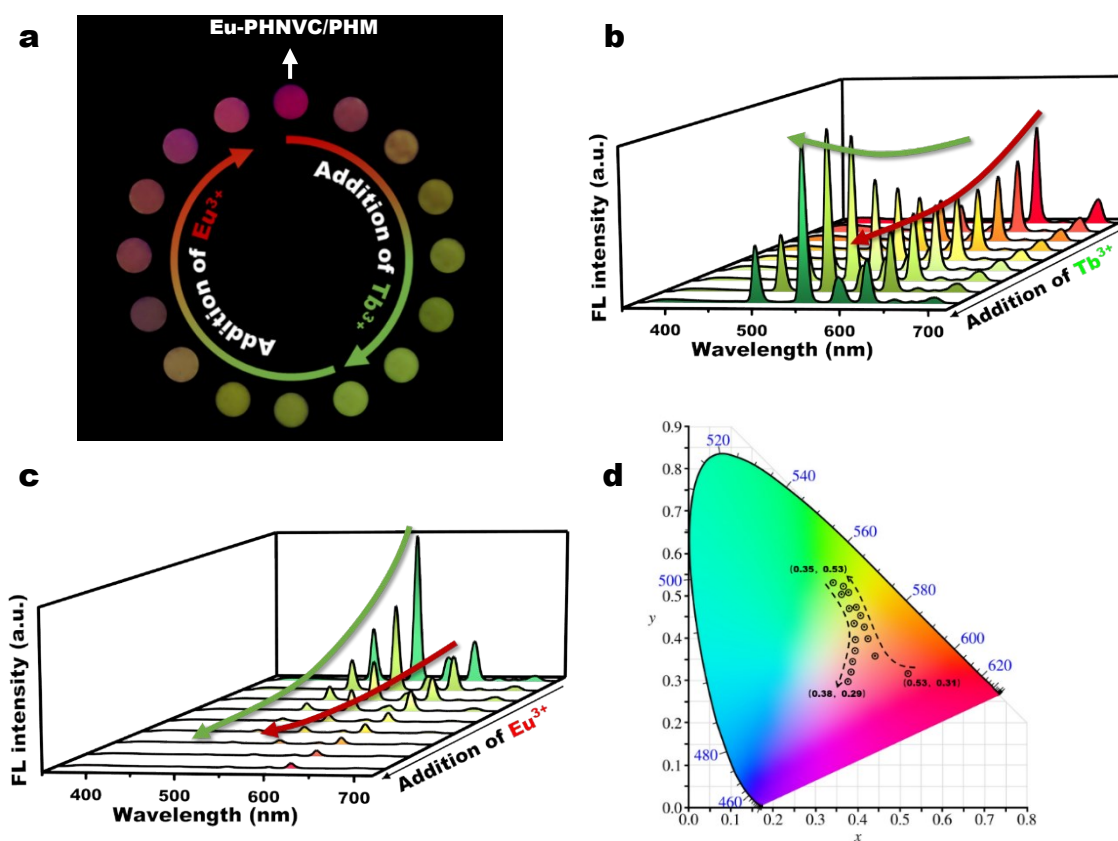


Figure S33. a) Digital photos showing the red-to-green color changing process of Eu-PHNVC/PHM from in response to Tb^{3+} stimulus, and the color recovery to red by further spraying the Eu^{3+} /methanol solution, as well as the corresponding fluorescence spectral change b-c) and the CIE coordinate change d). Excitation at 254 nm. All photos were taken under a 254 nm UV lamp.

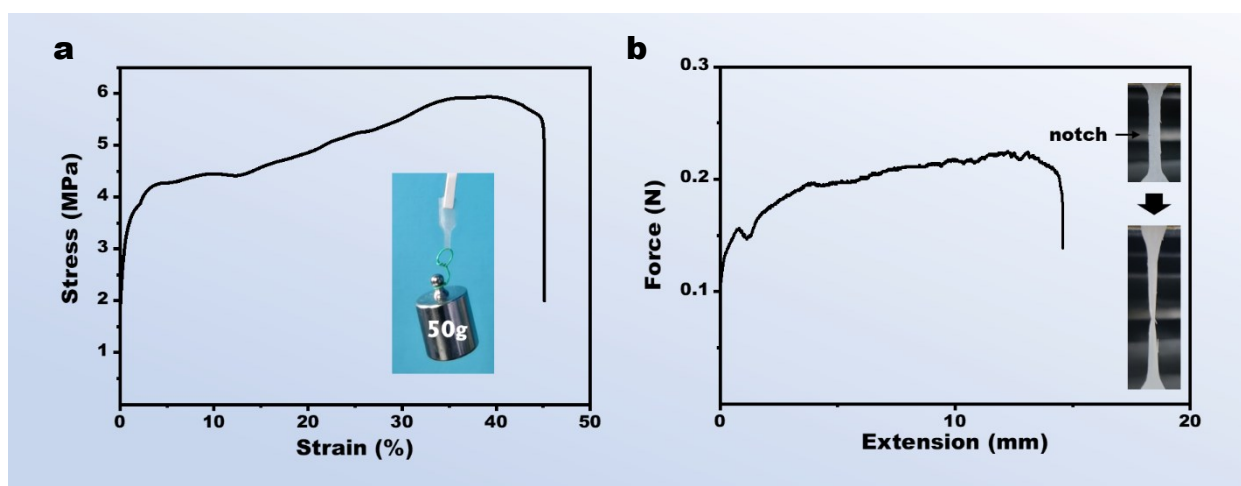


Figure S34. a) Strain–stress curve of the Eu-PHNVC/PHM film. Inset showing that the Eu-PHNVC/PHM film could withstand a 50 g weight. c) Tearing curve of Eu-PHNVC/PHM film.

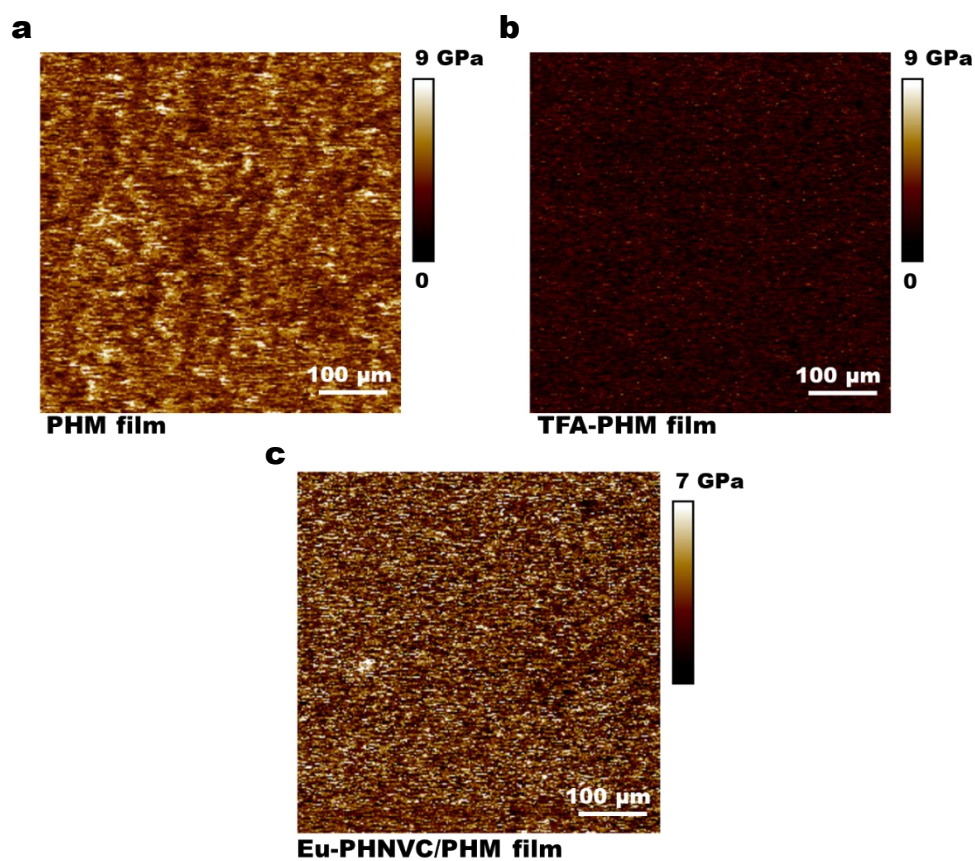


Figure S35. 2D Young's modulus distributions obtained by nanomechanical mapping of AFM for the PHM film (a), TFA treated PHM film (TFA-PHM film) (b) and the Eu-PHNVC/PHM film (c).

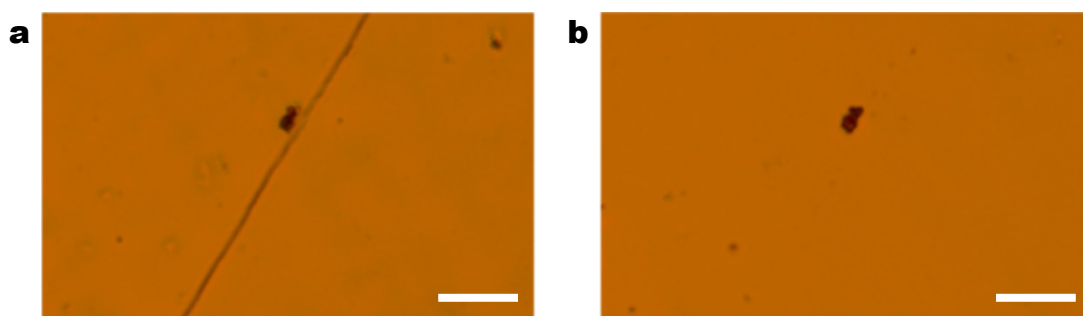


Figure S36. In situ microscopic image of Eu-PHNVC/PHM film before a) and after b) being self-healed in environment at RH=98% (Scale bars are 50 μm).

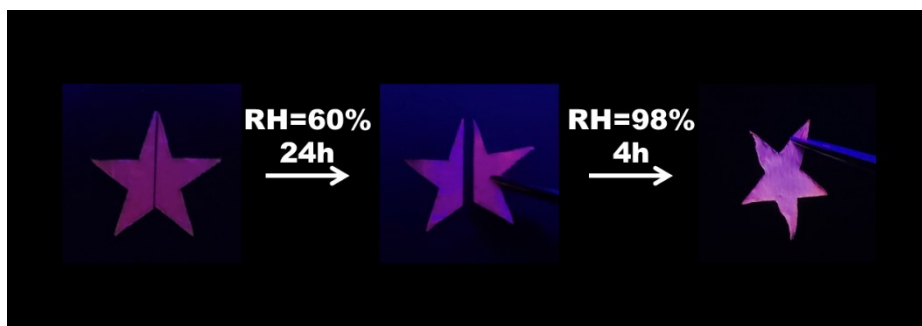


Figure S37. Results of trying to heal the broken Eu-PHNVC/PHM film under ambient humidity (RH=60%) for 24 h (a) and under high humidity (RH=98%) for 4 h (b). All photos were taken under a 254 nm UV lamp.

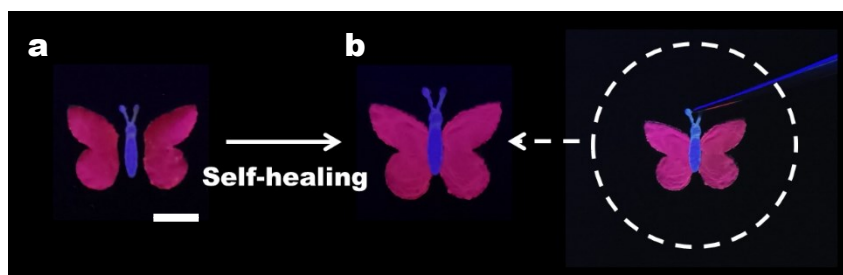


Figure S38. Digital photos showing the self-healing process of the man-made *morpho* butterfly (Scale bars are 5 mm). All photos were taken under a 254 nm UV lamp.

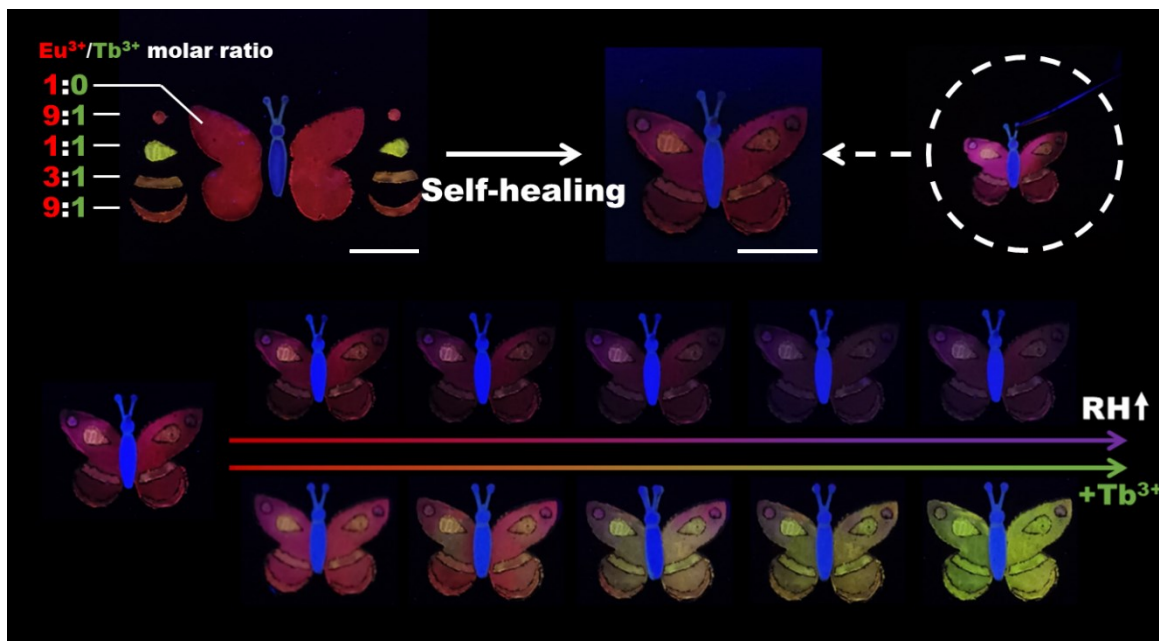


Figure S39. The artificial system designed to mimic the dazzling and colorful pattern change of the *morpho* butterfly (Scale bars are 5 mm). All photos were taken under a 254 nm UV lamp.

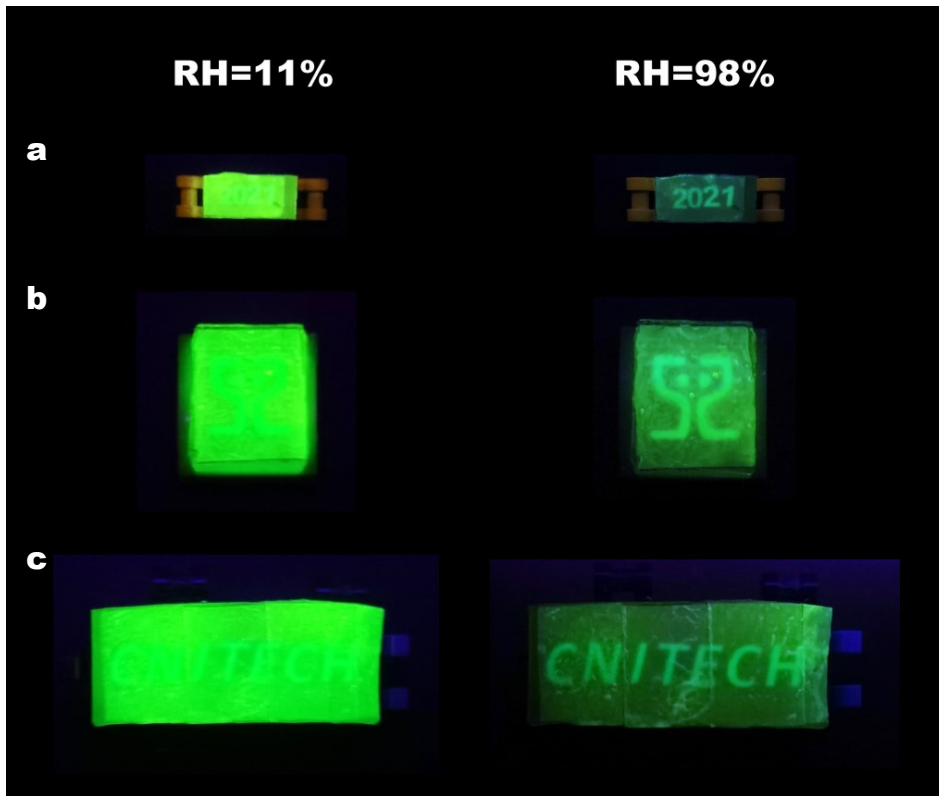


Figure S40. Digital photos of hiding (RH=11%) and display (RH=98%) of the information loaded on the tail a), head b), and back c) of the chameleon robot. All photos were taken under a 254 nm UV lamp.

3. Reference

1. R. B. Bai, J. W. Yang and Z. G. Suo, Fatigue of hydrogels, *Eur. J. Mech. a-Solid*, 2019, **74**, 337-370.
2. T. Gunnlaugsson, J. P. Leonard, K. Senechal and A. J. Harte, pH responsive Eu(III)-phenanthroline supramolecular conjugate: novel "off-on-off" luminescent signaling in the physiological pH range, *J. Am. Chem. Soc.*, 2003, **125**, 12062-12063.
3. M. P. Lowe, D. Parker, O. Reany, S. Aime, M. Botta, G. Castellano, E. Gianolio and R. Pagliarin, pH-dependent modulation of relaxivity and luminescence in macrocyclic gadolinium and europium complexes based on reversible intramolecular sulfonamide ligation, *J. Am. Chem. Soc.*, 2001, **123**, 7601-7609.
4. P. Chen, Q. Li, S. Grindy and N. Holten-Andersen, White-Light-Emitting Lanthanide Metallogels with Tunable Luminescence and Reversible Stimuli-Responsive Properties, *J. Am. Chem. Soc.*, 2015, **137**, 11590-11593.
5. D. Ghosh and N. Chattopadhyay, Characterization of the excimers of poly(N-vinylcarbazole) using TRANES, *J. Lumines.*, 2011, **131**, 2207-2211.
6. Y. Hu, L. Yang, Q. Yan, Q. Ji, L. Chang, C. Zhang, J. Yan, R. Wang, L. Zhang, G. Wu, J. Sun, B. Zi, W. Chen and Y. Wu, Self-Locomotive Soft Actuator Based on Asymmetric Microstructural Ti₃C₂T_x MXene Film Driven by Natural Sunlight Fluctuation, *ACS Nano*, 2021, DOI: 10.1021/acsnano.0c10797.
7. M. Amjadi and M. Sitti, High-Performance Multiresponsive Paper Actuators, *ACS Nano*, 2016, **10**, 10202-10210.